Hydro-Geophysical Evaluation of the Regional Variability of Senegal's Terrestrial Water Storage Using Time-Variable Gravity Data

Mohamed, Ahmed; Faye, Cheikh; Othman, Abdullah; Abdelrady, Ahmed

DOI
10.3390/rs14164059

Publication date
2022

Document Version
Final published version

Published in
Remote Sensing

Citation (APA)
Mohamed, A., Faye, C., Othman, A., & Abdelrady, A. (2022). Hydro-Geophysical Evaluation of the Regional Variability of Senegal's Terrestrial Water Storage Using Time-Variable Gravity Data. *Remote Sensing*, *14*(16), 1-19. Article 4059. https://doi.org/10.3390/rs14164059

remote sensing

MDPI

Article

Hydro-Geophysical Evaluation of the Regional Variability of Senegal's Terrestrial Water Storage Using Time-Variable Gravity Data

Ahmed Mohamed [1], Cheikh Faye [2], Abdullah Othman [3] and Ahmed Abdelrady [4,*]

[1] Geology Department, Faculty of Science, Assiut University, Assiut 71516, Egypt
[2] Geomatics and Environment Laboratory, U.F.R. Sciences and Technologies, Assane Seck University of Ziguinchor, Ziguinchor BP 523, Senegal
[3] Department of Environmental Engineering, Umm Al-Qura University, Makkah 24382, Saudi Arabia
[4] Faculty of Civil Engineering and Geoscience, Delft University of Technology, 2629 HS Delft, The Netherlands
* Correspondence: a.r.a.mahmoud@tudelft.nl

Abstract: The Gravity Recovery and Climate Experiment (GRACE) satellite data retrieval experiment has been instrumental in characterizing the global fluctuations in terrestrial water storage (ΔTWS) over the past 20 years. Given the limited availability of hydrological data, GRACE measurements are frequently combined with other climatic models, standardized precipitation index (SPI), and standardized temperature index (STI) data to examine the likelihood of such impacts on hydrology and calculate the groundwater storage changes (ΔGWS). The characterization of the intensity and variability of drought events has been identified based on the Terrestrial Water Storage Deficit Index (TWSI), derived from GRACE mass concentration blocks (mascons) over Senegal during the studied period (April 2002–December 2021). The results are: (1) The average annual precipitation (AAP) rate for the entire period was calculated at 692.5 mm/yr. (2) The GRACE-derived ΔTWS variations were calculated at +0.89 ± 0.34, +0.07 ± 0.36, +1.66 ± 1.20, and +0.63 ± 0.08 cm/yr for Periods I (April 2002–December 2009), II (January 2010–December 2017), III (January 2018–December 2021), and the entire period (April 2002–December 2021), respectively. (3) The ΔGWS changes were estimated to be +0.89 ± 0.31, +0.085 ± 0.33, +1.64 ± 1.11, and +0.63 ± 0.08 cm/yr for Periods I, II, II, and the entire period, respectively. (4) There is good agreement in some years and seasons according to the investigation of the link between the GRACE dataset, STI, and SPI. (5) Senegal's groundwater storage is increasing at a rate of 0.63 ± 0.08 cm/yr (1.24 ± 0.16 km^3/yr) between April 2002 and December 2021. (6) Considering the yearly extraction rates of 1.13 ± 0.11 cm/yr (2.22 ± 0.22 km^3/yr), an average recharge rate of +1.76 ± 0.14 cm/yr (+3.46 ± 0.28 km^3/yr) was calculated for the studied area. The integrated strategy is instructive and economical.

Keywords: geophysics; gravity; terrestrial water; groundwater monitoring; drought index; Senegal

Citation: Mohamed, A.; Faye, C.; Othman, A.; Abdelrady, A. Hydro-Geophysical Evaluation of the Regional Variability of Senegal's Terrestrial Water Storage Using Time-Variable Gravity Data. *Remote Sens.* **2022**, *14*, 4059. https://doi.org/10.3390/rs14164059

Academic Editors: Konstantinos X. Soulis, Jolanta Nastula and Monika Birylo

Received: 3 June 2022
Accepted: 15 August 2022
Published: 19 August 2022

1. Introduction

Fresh water is a resource that is not only vital but also essential for the preservation of the environment and socio-economic development. For an estimated quantity of water of 38.97 km^3/yr in 2017 [1] Senegal's renewable water resource potential is significant [2] and is distributed as follows: 36.97 km^3/yr in surface renewable water, and 25.8 km^3/yr in internal renewable water resources. In Senegal, the water dependency rate is 33.8%. Groundwater resources remain the country's main source of reliable and safe drinking water. Indeed, they are used both in rural and urban areas, for irrigated agriculture and livestock watering [3]. Industries and mines obtain water from groundwater [4].

Due to its significance, Senegal's groundwater needs to be managed sustainably because it is vulnerable to the effects of climate change and drought, which has become one of the country's most serious natural disasters in recent years due to low and infrequent

precipitation events and high evapotranspiration rates [5–10]. Extreme water scarcity always has disastrous effects on a country's people, crops, wildlife, and economy [11]. Droughts occur when precipitation is insufficient or nonexistent, leaving communities without enough water to sustain human and animal life. Improving water resource management and catastrophe avoidance is crucial since a drought disaster has long-lasting negative effects on a country's development that continue long after the drought itself has ended [12].

Although vulnerable to climate change, water resources are essential for society. Moreover, they are increasingly degraded by often unsustainable modes of use [13]. For better management of water resources, monitoring the evolution of terrestrial water storage changes (ΔTWS) in space and time remain a priority; hence the importance of using the Gravity Recovery and Climate Experiment (GRACE) tool, launched in 2002 [14–16], which has been used to observe the ΔTWS. ΔTWS is the total amount of water on the land's surface and in its subsurface. It consists of surface soil moisture, root zone soil moisture, groundwater, snow, ice, and water stored in vegetation, as well as river and lake water [17].

Because observational borehole data are scarce and spatial coverage is confined, research on significant changes in water storage is hindered [18]. A novel approach of satellite gravity has emerged in recent years to examine changes in spatial water storage because of the advantages of all-weather, high precision, and continuous space-time that these modern earth observation technologies (such as InSAR, GPS, and GRACE Gravity Satellites) have to provide [19–21]. From GRACE data, ΔTWS data can be extracted and used to characterize drought [22]. These data can therefore be used to calculate numerous drought indices which will make it possible to quantify the hydrological conditions of an environment, its humidity conditions, its deficiencies, or its excesses of water [23]. This research has substantially improved our understanding of flood-related hydrologic events (e.g., [24,25]), droughts (e.g., [26,27]), groundwater storage variability and recharge and depletion rates of aquifer systems (e.g., [28–43]), and evapotranspiration [44]. To obtain the groundwater storage changes (ΔGWS) trend value, the non-groundwater components should be subtracted from the ΔTWS. Regional canopy water (ΔCWS), snow water equivalent (ΔSWE), soil moisture (ΔSMS), surface water (ΔSWS), and groundwater reserves make up regional water storage from a vertical layering view [45]. GRACE is unable to distinguish between the contributions made by the different ΔTWS compartments (such as ΔSWS, ΔSWE, ΔSMS, and ΔGWS). By combining the outputs of land surface models with GRACE data, it is possible to find out more about specific parts of the ΔTWS estimates from GRACE and to increase the horizontal resolution of the data. Outputs of the Global Land Surface Assimilation System (GLDAS; [16,46,47]) were used to separate the ΔTWS into its parts.

For the characterization and monitoring of drought and flood conditions and changes in water storage, many authors have used GRACE data [48–50]. Following the noted changes in ΔTWS from GRACE data, drought indices have been developed [51]. Hydrological drought can be measured in terms of when it began, how long it lasted, and how severe it was, all with data from the GRACE satellites [52]. GRACE's generated ΔTWS appears to have a high correlation with rainfall indices throughout most regions. There is a correlation between drought characteristics based on GRACE and the results of the Standardized Precipitation Index (SPI) and Standardized Temperature Index (STI) in some areas [53], hence the importance of including these two climatic drought indices which use the precipitation and evapotranspiration in hydrological studies [54].

A good concordance between drought indices and GRACE-derived ΔTWS data was utilized to validate and demonstrate the significance of all these data for drought predictions in specific areas [50,55]. Our current study of the ΔTWS in Senegal makes use of GRACE and GRACE Follow-On (GRACE-FO) data and highlights the connections between the ΔTWS's spatiotemporal variability and changes in the SPI and STI. Moreover, we have estimated the mass variation in groundwater storage caused by natural effects and/or manmade activities in Senegal. To examine how climatic variability affects variations in

groundwater storage in the study area, data from the Tropical Rainfall Measuring Mission (TRMM) were utilized to derive the main rainfall patterns over Senegal.

2. Study Area

Senegal, a nation that borders the North Atlantic, is situated in the far western part of Africa between latitudes 12°8′ and 16°41′ North and the longitudes 11°21′ and 17°32′ West (Figure 1). It has an area of 196,722 km^2. Senegal has a Sudano-Sahelian climate and is situated in a tropical region.

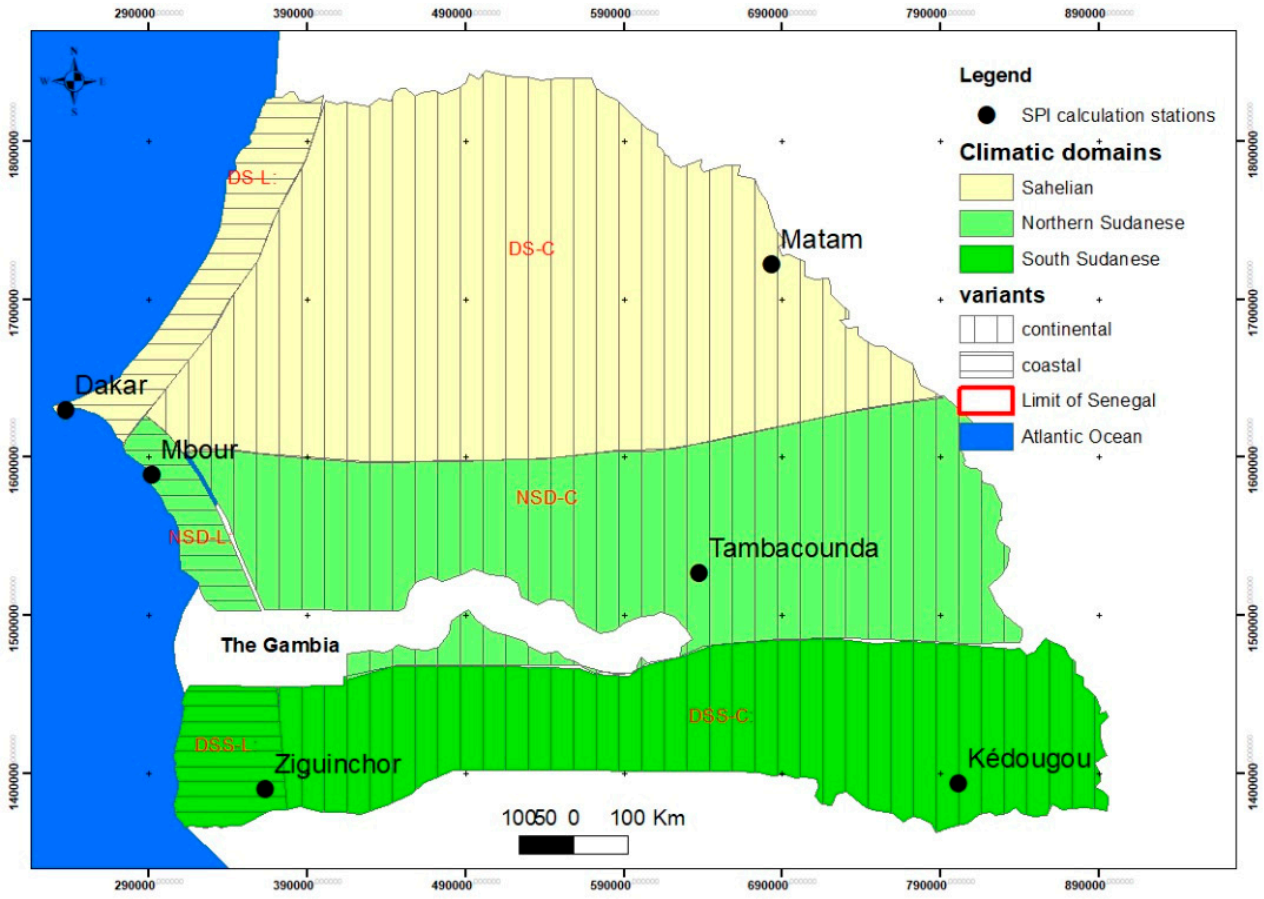

Figure 1. Location map of the study area showing the climatic stations.

On average, annual rainfall varies from north to south, from 200 mm (Sahelian domain) to around 1250 mm (southern Sudanian domain [10]. Senegal has, depending on rainfall, three climatic domains: the Sahelian, northern Sudanese, and southern Sudanese domains (Figure 1).

Senegal has a wide range of climates, from the desert (Sahelian) in the north to tropical in the south. There are two different periods in the year: a dry season, with continental trade winds and mild temperatures, from November to May, and a wet season with high temperatures and monsoon rains from June to October, which is called "wintering".

According to reports, the severe droughts have altered the region's water and heat conditions visibly, decreased the amount of drinking water available to locals, interfered with the operation of the vegetation service, and even reduced biodiversity and degraded flora [10]. As a result, it is crucial to characterize the humidity levels in Senegal to manage the risks associated with the spatiotemporal variability of water resources as well as agricultural and pastoral outputs. It also has the benefit of giving an early warning to safeguard the ecological environment. The repercussions of this drying phenomenon are considerable, particularly in the agricultural field, and they have led farmers to reorganize

their traditional cropping systems to better adapt them to more arid conditions. This adaptation is all the more necessary, as the deterioration of the total rainfall is only one part of the range of data that must be taken into account.

Surface and groundwater have tremendous potential as water resources in Senegal. The Gambia, Kayanga, and Senegal rivers, which have their sources in Guinea, hydrate a sizable portion of the nation. Senegal, therefore, has a fairly varied and abundant hydrological potential. The majority of the surface water reserves are found in the Gambia and Senegal river basins, which receive their water from the Republic of Guinea's Fouta Djallon mountain [56]. There are minor streams with sporadic flows that run alongside these two big rivers. These include Casamance, Kayanga, with the Anambé as its principal tributary, Sine, Saloum, and the coastal backwaters. This hydrographic network is completed by the ponds in the Niayes region of the northern coast, Lake Guiers, the bolongs of the estuary areas, and Ferlo.

Since the beginning of the drought, groundwater has become even more of a significant factor in Senegal's water potential. The four primary aquifer systems in the nation are the superficial aquifer system, the intermediate aquifer system, the deep aquifer system, and the bedrock aquifer system. They correlate to the four main geological formations.

3. Data and Methods

3.1. Gravity Data

To analyze the variations of ΔTWS, and to estimate the ΔGWS changes in Senegal, the GRACE processing center's three-time variable gravity mascon solutions were analyzed. The mascon products are reflected in the CSR-RL06M v02, JPL-RL06M v02, and NASA Goddard Space Flight Center (GSFC)-RL06M v01 databases, respectively. These mascon solutions catch all impulses within the GRACE noise limits with superior spatial resolution and less uncertainty than spherical harmonic solutions. There is no need for smoothing or destriping. Additionally, the scaling factor might not be necessary for some products [57–60].

ΔTWS anomalies were computed for each 3° × 3° spherical cap mascon block in the JPL-RL06M v02 solution to ensure that all blocks were of comparable size [58,59]. All ΔTWS changes in the final dataset are sampled on a longitude-latitude grid of 0.5° × 0.5°. Leakage signals induced by 3° mascon blocks can be recovered using the JPL-provided scaling factors, assuming the JPL-RL06M v02 has a true 3° resolution. Separating land and sea mascons is easier with the JPL-RL06M v02 data. Using the Coastal Resolution Improvement filter [58] on the full mascon solution helps to separate land masses from mascons that traverse coastlines and reduces leakage errors at coasts [59].

ΔTWS variations for 0.25° × 0.25° longitude-latitude grids are displayed in the CSR-RL06M v02 solution, which was derived from an equal region with a resolution of 1° [60,61]. This new grid features hexagonal tiles that isolate the ocean from the land, helping to minimise signal loss. The scaling factor is not required for these tiny mascons. In addition to the CSR and JPL mascon datasets, the GSFC-RL06v1.0 mascon solution [62] was used. The GAD product has been reinstated in this global mascon solution, so the ocean mascons now depict ocean bottom pressure. This item is comparable to those from JPL and CSR mascon products. ΔTWS anomalies were computed for each equal-area 1° × 1° square mascon [57]. The 1-arc-degree equal area values have been arranged on a 0.5° × 0.5° grid with equal angles. While ocean values have been interpolated or extrapolated, land values are determined using a least squares estimator that preserves mass throughout each region.

In response to the frequency and severity of extreme climate change, these measurements by GRACE represent the total amount of water stored above and below ground [50,63]. In addition, the terrestrial water storage deficit (TWSI) based on GRACE data is defined as follows [49]:

$$\mathrm{TWSi.j} = \mathrm{TWSAi.\,j} - \overleftarrow{\mathrm{TWSAj}} \quad (1)$$

where $TWS_{i\cdot j}$ is the time series inferred from GRACE (TWSAi. j) for month j of year i, and $\overleftarrow{TWSAj}$, is the long-term average (January 2003–December 2021) of the TWSA for the same month in one year. When compared to its typical monthly values, the terrestrial water storage value is either positive or negative, with the former indicating excess storage [49]. We normalized this parameter to produce an index of overland water storage (TWSI) defined in Equation (2), which enables us to compare TWS with other drought indices and better characterize droughts based on it.

$$TWSI = \frac{TWS - \mu}{\sigma} \quad (2)$$

where μ is the mean and σ is the standard deviation of the TWS time series. The time series of TWSI values represent the mean deviation from the conditions of the area and its magnitude indicates the intensity of the drought. GRACE data were utilized to display the water storage deficit on a yearly time scale [50].

The monthly data, that was missing was, interpolated using the cubic-spine method. The current study made use of the mascon solutions throughout the investigation. The trends' slope values of ΔTWS were calculated. The errors connected to the estimated trend values were then calculated.

3.2. Groundwater Storage Change

The non-groundwater components (ΔSMS, ΔCWS, and ΔSWE) are estimated using the GLDAS [64] outputs. In the current work, estimation and application of the averaging of three GLDAS models (VIC, NOAH, and CLM) were made to estimate the ΔGWS by subtracting the fluctuations in the non-groundwater components from the ΔTWS.

3.3. Rainfall, and Temperature Data

A cooperative space effort called TRMM was designed to track and study tropical rainfall [65]. The average annual precipitation (AAP), and the monthly rainfall time series are produced across the study area using the monthly TRMM data, which cover the period from January 2002 to December 2019 with a spatial resolution of $0.25^\circ \times 0.25^\circ$.

This study also employed temperature data from the Agence Nationale de l'Aviation Civile et de la Météorologie stations in Kédougou, Ziguinchor, Tambacounda, Mbour, Dakar, and Matam, which are sufficiently representative of the country's diverse climatic areas. The SPI and STI indices are computed using the average monthly precipitation and temperature datasets.

3.4. Standardized Drought Indices

Typically, standardized indicators are used to express and describe drought phenomena. We employed two types of meteorological and/or drought indicators, the SPI and the STI, to define droughts in Senegal and compare them to the TWSI produced from GRACE data [66]. The SPI is an index that is powerful, flexible to use, and simple to calculate. Rainfall data is the only required parameter. Additionally, the SPI index can be used to analyze both rainy and dry periods or cycles. Many drought planners appreciate the flexibility of the SPI index. The index is also used in various research institutes, universities, and National Meteorological and Hydrological Services around the world for drought monitoring and early warning activities. It is possible to calculate the index for various time scales, allowing drought situations to be detected quickly and their severity to be assessed [67], and is less complex than many other indices, in particular the Palmer drought index. It is given by the following Equation (3):

$$Pi = \sigma\, SPI + \mu \quad (3)$$

where Pi is the precipitation, μ is the mean and σ is the standard deviation of the precipitation time series.

Because of its flexibility and usability, the SPI can be used to characterize drought patterns in Senegal and serve as a reference point for their mitigation, local water resource management, and agricultural decision making [68]. The STI is an expansion of the SPI that substitutes temperatures for precipitation in its calculation. It is given by the following Equation (4):

$$Ti = \sigma STI + \mu \quad (4)$$

where Ti is the temperature, μ is the mean and σ is the standard deviation of the temperature time series. The STI index is often used to spatially characterize climate change.

4. Result and Analysis

4.1. Analysis of ΔTWS Trends

The three separate solutions of GRACE-derived ΔTWS trends show an overall increase between 2003 and 2021 across the country (Figure 2). The GRACE-derived ΔTWS calculated from the CSR, JPL, and GSFC mascons showed gain rates of +0.63 ± 0.12, +0.54 ± 0.07, and +0.76 ± 0.08 cm/yr, respectively (Table 1). There are good agreements between the ΔTWS extracted from the various sources in terms of amplitude, phases, and trends, with a correlation of 0.89 to 0.97. The average ΔTWS of the three different solutions is +0.63 ± 0.08 cm/yr (Figure 2, Table 1). The increasing trends are statistically significant at the 99.9% confidence level for the three mascon datasets and on the different climatic domains (Figure 1; DSS-L: Coastal Southern Sudanian Domain; DSS-C: Continental Southern Sudanian Domain; NSD-L: Coastal Northern Sudanian Domain; NSD-C: Continental Northern Sudanian Domain; DSS-L: Coastal Sahelian Domain; DSS-C: Continental Sahelian Domain). In each climatic domain, the trend value is higher in the continental variant (DSS-C: 0.330; DNS-C: 0.399; DS-C: 0.337) than in the coastal variant (DSS-L: 0.294; DNS-L: 0.398; DS-L: 0.232). Between the climatic domains, the trend values in the South Sudanian domain are lower than those of the North Sudanian domain but generally higher than those of the Sahelian domain.

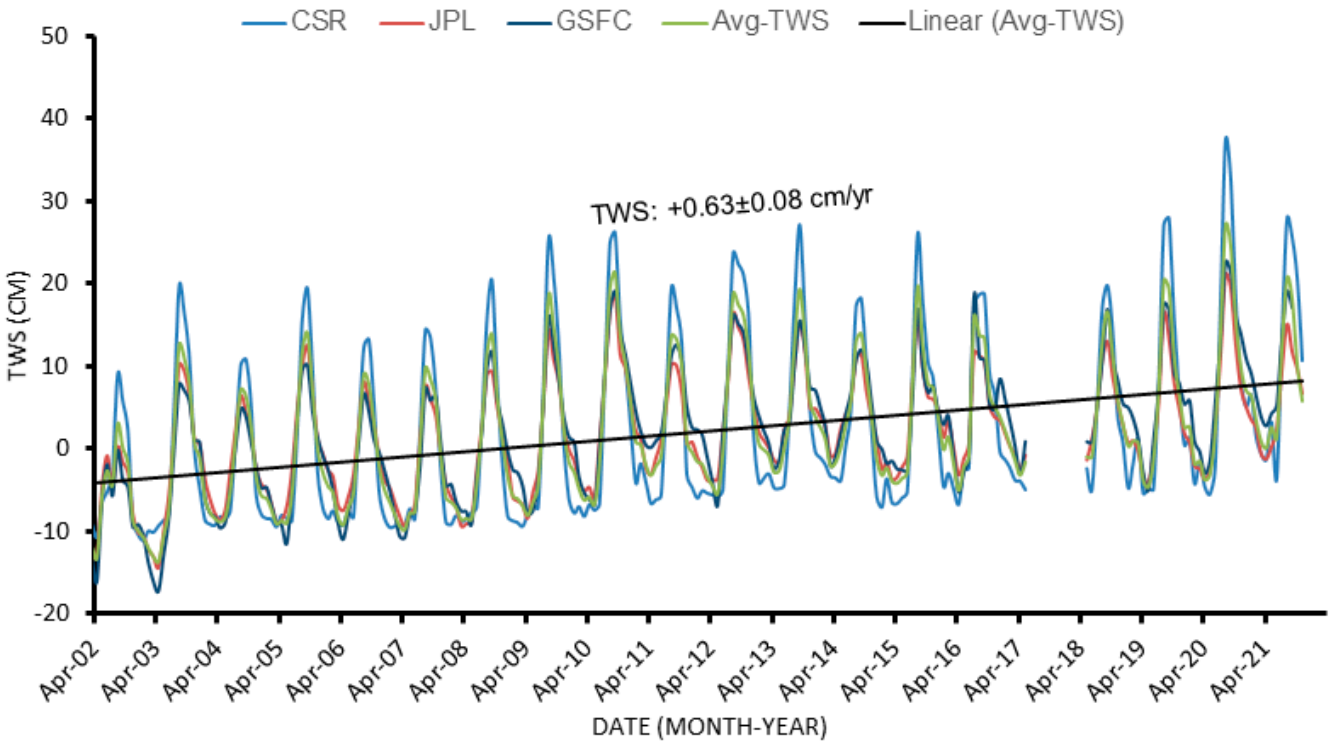

Figure 2. Monthly time series of the ΔTWS from the different GRACE sources and their averaging (Avg-TWS) over the study area during the entire period.

Table 1. GRACE-derived ΔTWS components (cm/yr) over the study area at 95% confidence level.

Component		Entire Period	Period I	Period II	Period III
GRACE total (ΔTWS)	CSR	+0.63 ± 0.12	+0.69 ± 0.44	+0.18 ± 0.50	+2.78 ± 1.72
	JPL	+0.54 ± 0.07	+0.80 ± 0.29	+0.05 ± 0.29	+1.13 ± 0.95
	GSFC	+0.76 ± 0.08	+1.17 ± 0.30	+0.011 ± 0.30	+2.04 ± 1.08
	AVG	+0.63 ± 0.08	+0.89 ± 0.34	+0.07 ± 0.36	+1.66 ± 1.20
ΔSMS		−0.002 ± 0.01	0.004 ± 0.003	−0.013 ± 0.042	0.022 ± 0.132
ΔGWS		+0.63 ± 0.08	+0.89 ± 0.31	0.085 ± 0.33	+1.64 ± 1.11
AAP (mm)		692.5	696.1	696.1	645.8

CSR, JPL, and GSFC: mascon products; ΔTWS: changes in Terrestrial Water Storage; ΔGWS: Groundwater Storage Change; ΔSMS: Change in soil moisture; AAP: Annual Average Precipitation.

The southern and southwestern sections of the examined area are experiencing significantly positive ΔTWS trends, whereas the northern and northeastern parts are experiencing comparatively modest positive ΔTWS trends, as shown by the geographical distribution of the secular ΔTWS trends (Figure 3). Based on a linear regression analysis of their average, the ΔTWS variation time series exhibits three distinct trends with various slope values during the entire analyzed period (Figure 4). The beginning trend (Period I) exhibits an estimated +0.89 ± 0.34 cm/yr somewhat positive trend (Table 1). For the second trend (Period II), a positive trend of +0.07 ± 0.36 cm/yr is expected. The third trend (Period III) exhibits a marginal increase with an estimated annual rate of +1.66 ± 1.20 cm/yr.

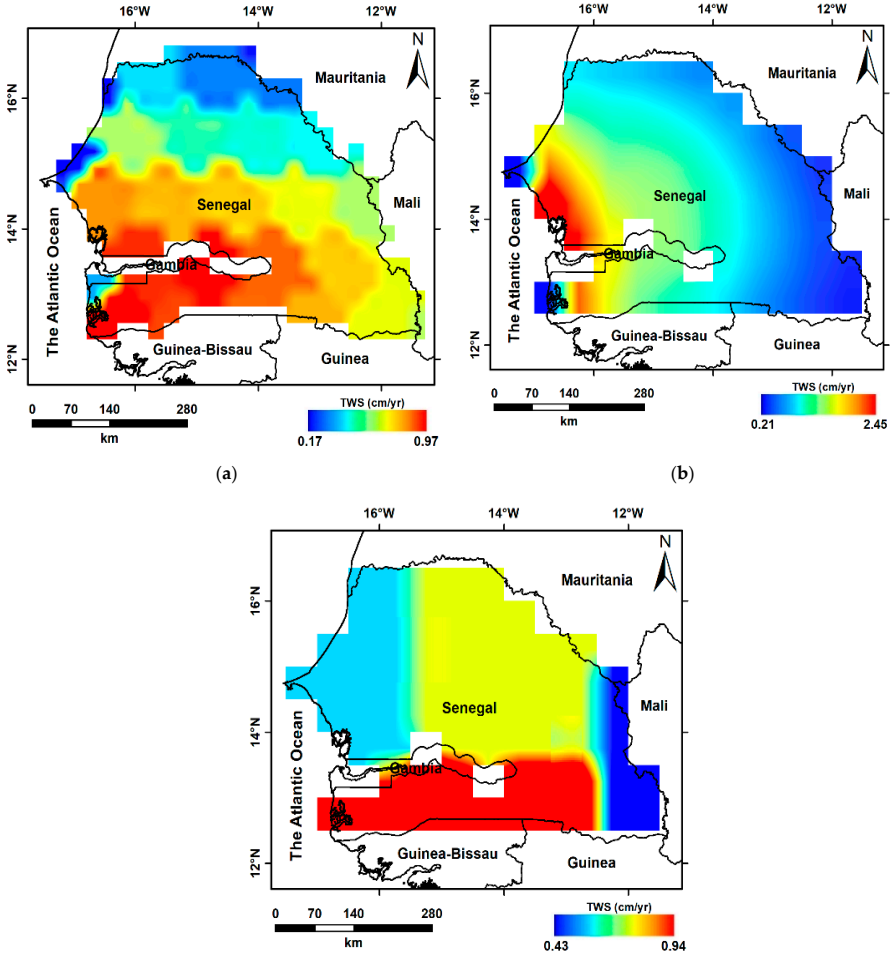

Figure 3. A color-coded secular extracted ΔTWS trend map for Senegal was derived by averaging the monthly CSR (**a**), GSFC (**b**), and JPL (**c**) products over the country.

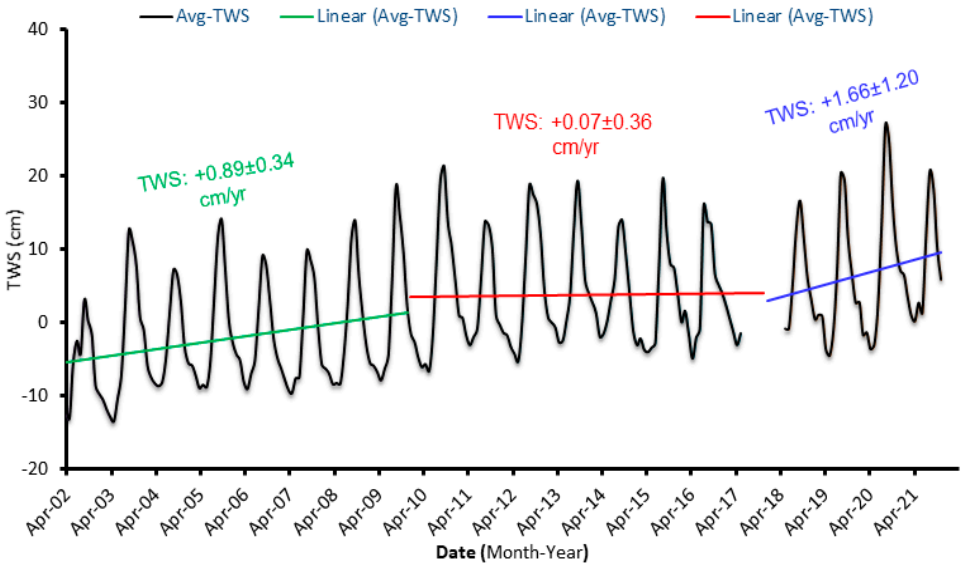

Figure 4. Monthly time series of the Avg-TWS over the study area during the three periods.

4.2. Analysis of the Groundwater Storage Variation from GRACE

Figure 3 reveals that during the examined time, the southern sections of the study area are showing higher positive ΔTWS trend values, whereas the northern and eastern parts of Senegal are experiencing lower positive ΔTWS trend values. This is because the southern part receives a lot more rain than the northern part as shown in Figure 5a, which displays the average annual precipitation rate over the study area. The measured changes in the mean monthly rainfall are shown through time in Figure 5b. During the examined period, the solutions generated from CSR, JPL, and GSFC exhibit increasing trends estimated at +0.63 ± 0.12, +0.54 ± 0.07, and +0.76 ± 0.08 cm/yr, respectively. The average ΔTWS is calculated to be +0.63 ± 0.08 cm/yr (Table 1).

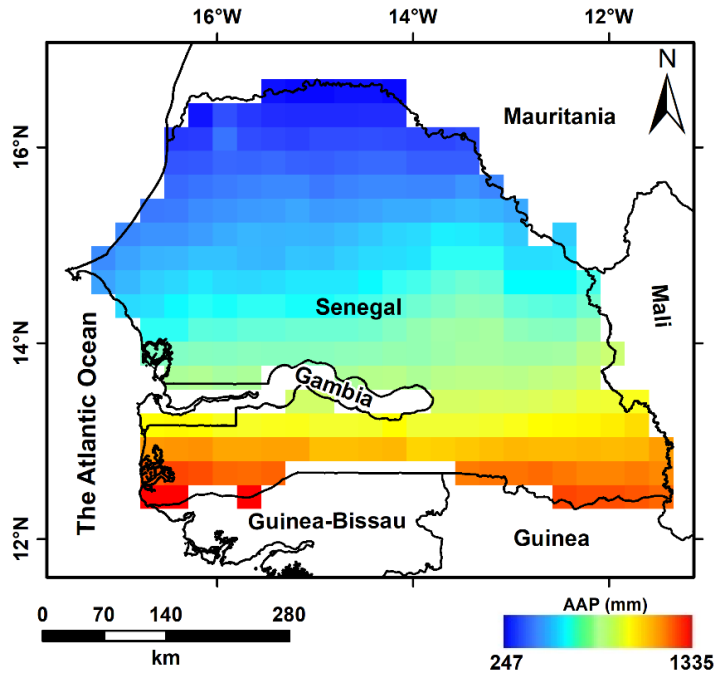

(**a**)

Figure 5. *Cont.*

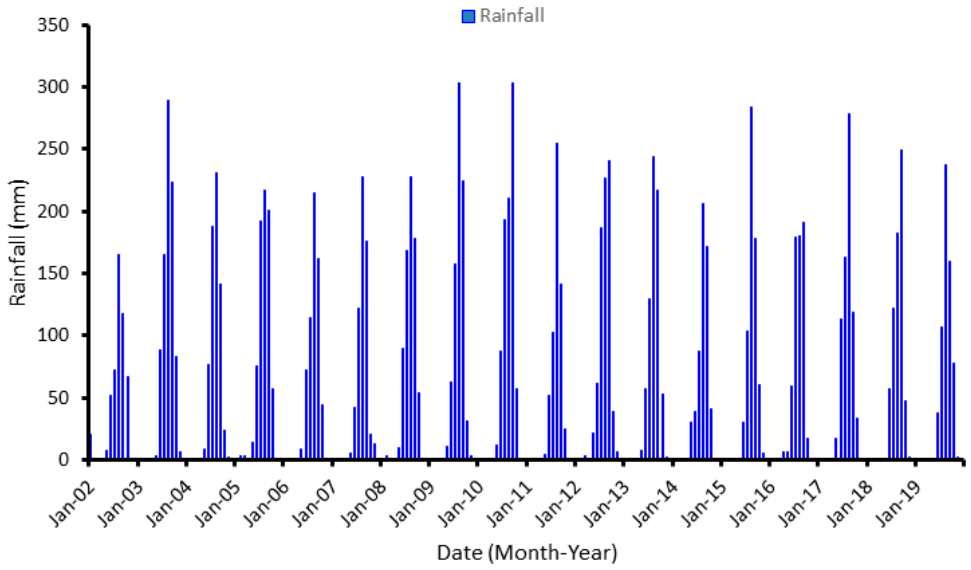

(**b**)

Figure 5. (**a**) The AAP extracted from TRMM data over the study area. (**b**) Monthly rainfall over the study region during the entire period.

Three GLDAS models (VIC, NOAH, and CLM) were used to estimate the trend in the GLDAS-derived ΔSMS, ΔSWE, and ΔCWS trends. The ΔSWE and ΔCWS show no trends, however, the average ΔSMS was determined to be -0.02 ± 0.01 mm/yr, showing a very slight negative trend during the entire period (Figure 6; Table 1).

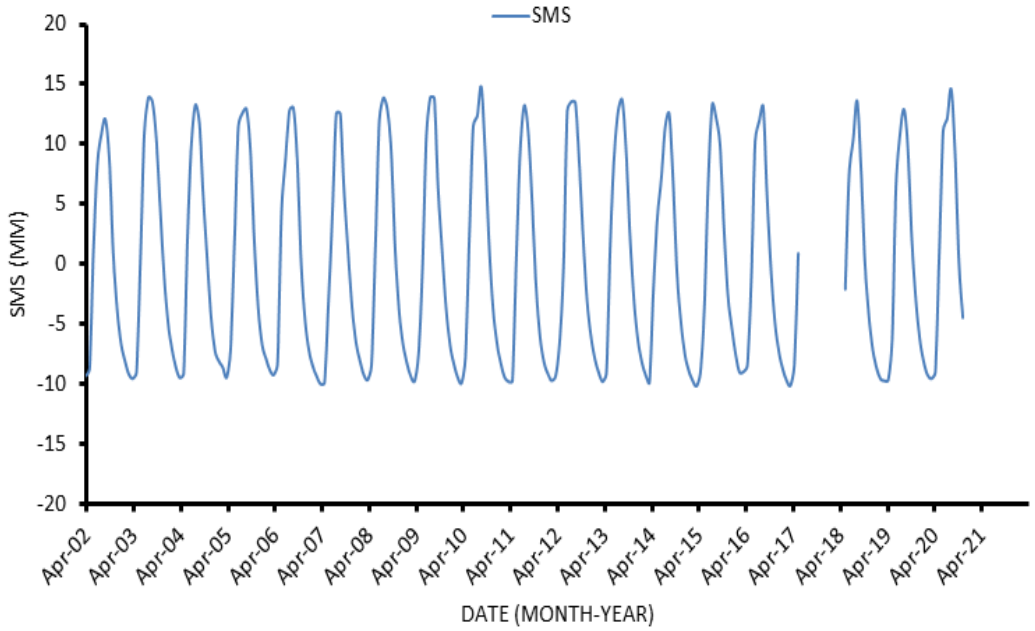

Figure 6. GLDAS-derived ΔSMS in Senegal during the entire period.

By subtracting the ΔSMS trend from the ΔTWS using following Equation (5). The trend in average ΔGWS was estimated to be $+0.63 \pm 0.08$ cm/yr during the entire period.

$$\Delta TWS = \Delta GWS + \Delta SMS + \Delta SWE + \Delta CWS \quad (5)$$

The ΔGWS time series (Figure 7) exhibits fluctuations that are somewhat resemblant to those of the ΔTWS time series with an increasing trend of +0.63 ± 0.08 cm/yr during the entire period. A slightly increasing trend was estimated to be +0.89 ± 0.31 cm/yr throughout period I (Figure 8). It has a little positive trend, estimated to be +0.085 ± 0.33 cm/yr during Period II (Table 1). Finally, period III shows a considerably positive ΔGWS trend of +1.64 ± 1.11 cm/yr.

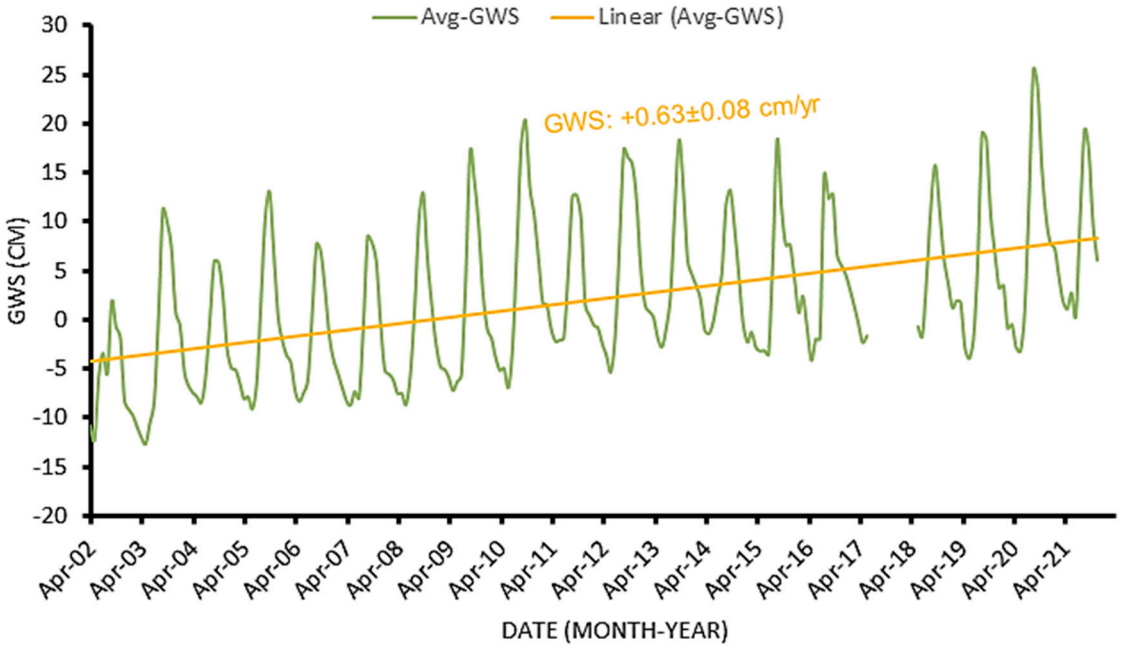

Figure 7. Monthly variation of the Avg-GWS in the Senegalese territory.

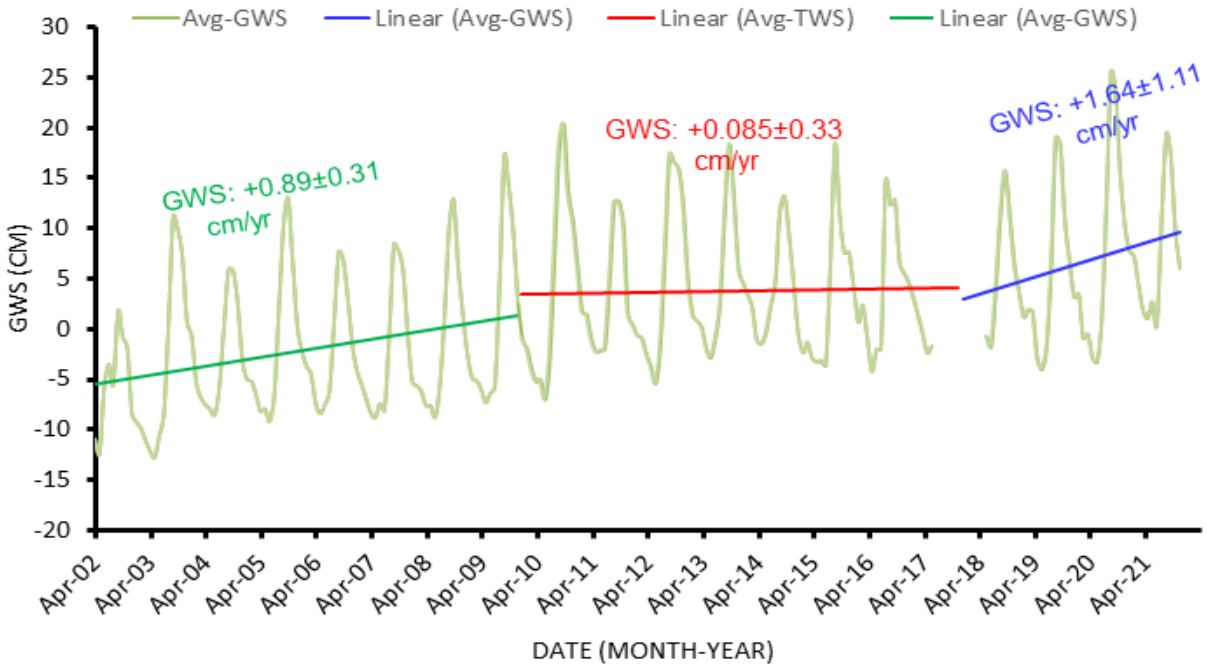

Figure 8. Monthly time series of the Avg-GWS over the study area during the three periods.

4.3. Investigation of the Relationship between Drought Indices and GRACE Data

The temporal fluctuations in ΔTWS, precipitation, and temperature from 2003 to 2021 are depicted in Figure 9a,b. Precipitation and TWS generally show an upward trend from

2003 to 2021 and have a good correlation. Between 2003 and 2021, Senegal's average water storage increased at a rate of +0.63 ± 0.08 cm/yr, but precipitation increased only at a low rate of +0.105 mm/yr. Precipitation evolved at a rate of 0.29 mm/yr in Ziguinchor, 0.01 mm/yr in Kédougou, 0.2 mm/yr in Mbour, and 0.14 mm/yr in Dakar, then decreased until negative values in Tambacounda (−0.14 mm/yr) and Matam (−0.09 mm/yr). Similar trends were noted for temperatures which increased by 0.29 °C/yr in Ziguinchor, 0.45 °C/yr in Kédougou, 0.20 °C/yr in Tambacounda, and 0.56 °C/yr in Matam. Thus, it will be a question of noting, according to the characterization of an episode of drought [50], the existence of droughts relating to the storage of terrestrial water that can reach 10 months during the period 2003–2021 in Senegal.

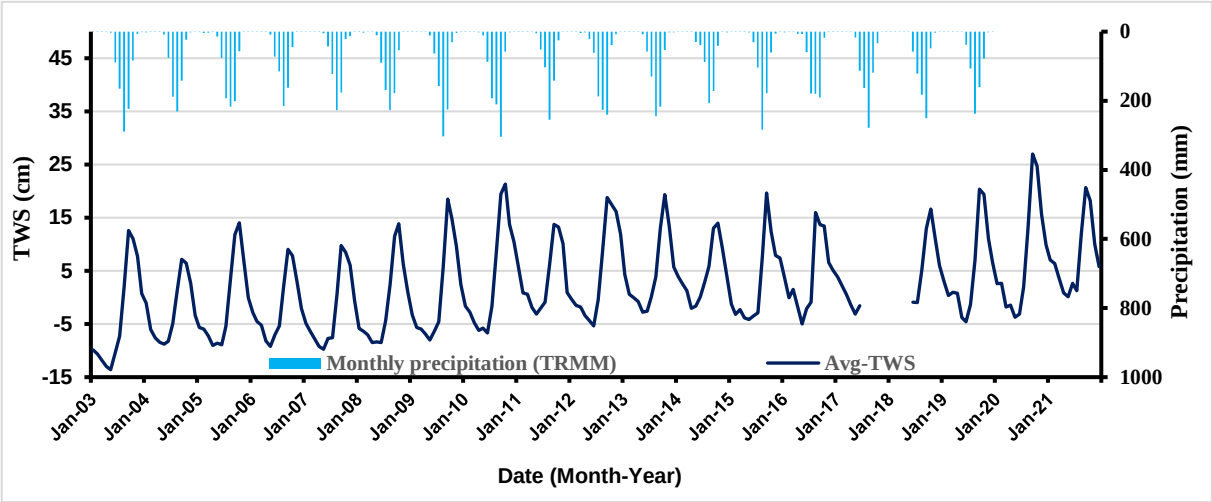

(**a**)

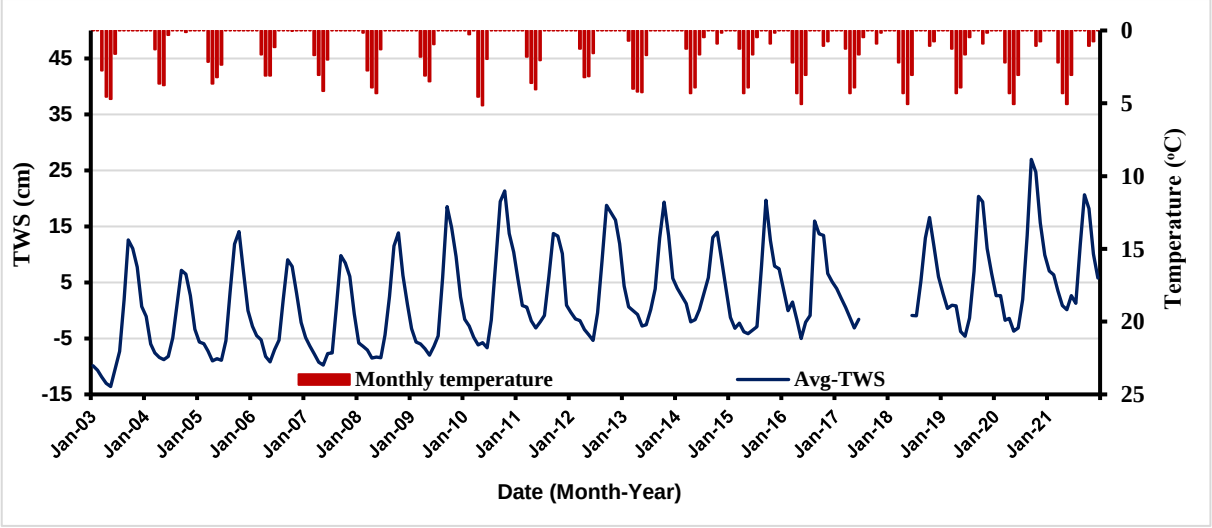

(**b**)

Figure 9. Evolution of precipitation and GRACE-derived ΔTWS anomaly (**a**), and Evolution of mean temperature anomaly and GRACE-derived ΔTWS anomaly (**b**) from 2003 to 2021 in Senegal.

According to CSR data, the driest years had 4 to 6 deficit months. The two worst drought years in the nation, with corresponding durations of 6 months, occurred in 2003 and 2007. The most severe drought events, which occurred in November 2003 and 2007, had deficit peaks of −2.819 cm and −1.227 cm, respectively. However, the period between 2011 and 2021 is still unique because it did not record a single month with a deficit.

According to JPL information, the droughts were more intense, and the driest years had 6 and 10 deficit months. The two worst drought years in the nation, with corresponding lengths of 10 and 6 months, were 2003 and 2004. The most severe drought episodes, which occurred in January 2003 and February 2004, had deficit peaks of −12.029 cm and −13.168 cm, respectively. Even throughout the rainy years of 2010 to 2021 in this series, there was at least one dry month every year.

The drought is the worst of all the series for the GSFC data, and there can be as many as 11 months with a deficit. The country experienced its two worst droughts in 2003 and 2004, which lasted 11 and 6 months, respectively. The most severe drought episodes, which occurred in February 2003 and 2004, had deficit peaks of −14.411 cm and −15.632 cm, respectively. Unlike the JPL series, the GSFC data, during at least two years (2012 and 2019), had no deficit months.

5. Discussion

To identify regional groundwater storage anomalies in the Senegalese territory, an integrated approach was chosen to detect, assess and quantify their variability. This approach has therefore greatly helped in understanding the hydrological changes [69,70] and has made it possible to assess groundwater variation in Senegal. Through our results, we note a correlation between the anomalies of the storage based on GRACE data and the SPI and STI indices which make it possible to characterize the drought and its impact on the availability of groundwater.

Previous global assessments of groundwater stress have been hampered by uneven and variable estimates of usage and availability [71,72], which raises serious concerns about determining groundwater sustainability. Although surface water is becoming less dependable and unpredictable, groundwater continues to be the primary source of water for agriculture [73], and its significance is growing quickly as it is stored as a source of supply. Based on the evolution of the ΔTWS data, the results highlight the variations in ΔTWS in Senegal and show an increase in ΔTWS estimated at +0.63 ± 0.08 cm/yr across the entire country during the study period. With the removal of the soil moisture storage variation from the ΔTWS, the ΔGWS is estimated at +0.63 ± 0.08 cm/yr. The GRACE-derived ΔTWS trend indicates a marginal improvement in Senegal's groundwater. Our findings represent a step in the development of strategies for the expectation of the Sustainable Development Goals proposed by the United Nations [74]. The various changes in the availability of groundwater resources are most likely attributed to human pressures, as well as climate change and variability, as captured by GRACE.

Although GRACE is a tool for monitoring variations in groundwater storage around the world and makes it possible to compensate for the lack of data due to the rarity of hydrometeorological sites [75], the uncertainties linked to the results of GRACE are still very high and should be carefully assessed [76]. The fact that the GRACE satellites are in polar orbit and that there are faults in the GRACE payload observation cause systematic errors and random noise in the GRACE resolutions. When it comes to monthly water storage estimations, GRACE is unable to distinguish between different hydrological storages [77]. Additionally, because the average monthly water storage is not precise enough for short periods, it is difficult to predict the variability in water storage. To remedy this [50] suggested there should be a preference to choose long time series. Several scientists have opted to create separation techniques as a response to the GRACE errors found in the satellite's ΔSMS, GRACE measurements, processing, and leakage [78,79]. However, using the GRACE mascon solutions released by JPL, CSR, and GSFC and their averaging helped to overcome these errors. These mascon systems provide better spatial resolution and lower inaccuracy in capturing all signals within the GRACE noise levels. There is no need for smoothing or destriping. Additionally, the scaling factor might not be necessary for some products [57–60]. Other satellites and aerial geophysical field datasets have been recently used to investigate continental-scale crustal characteristics [80], magma chamber geometry, and heat flow [81], and land subsidence due to significant groundwater extraction [82].

In more limited contexts, however, geophysical data from the air and the ground have been utilized to investigate things such as underground water systems and subsurface geology [83,84].

The analysis of the relationship between the GRACE dataset, STI, and SPI for some regions is shown in Table 2. Some certain variations in behavior were noted because these indices were created using various factors and approaches. As a result, the storage levels in some months, seasons, and years do not correspond to the evolution of the climate indices. For instance, in some years, such as 2003, 2007, 2012, and 2015, the water storage index was lower than the other indices, while in other years, it was often greater than the other three indices. The STI and SPI indices (Figure 10) exhibit high levels of variability and nearly comparable changes over the course of the study period reflecting dry and/or hot episodes. In this analysis, dry or hot periods were determined to be those that included at least one low-precipitation or high-temperature data. The standards for identifying the start and end of a drought event were set by [66]. When the SPI is consistently negative and drops to a value of −1 or less, a drought event starts. When the SPI value changes to positive, the event is over. Although the water storage deficit can be used to estimate how much water is needed, it is unable to distinguish between variations in water deficit intensity. The water storage index's behavior and response to climatic anomalies, in general, were in reasonable accord with the other indicators tested in this study.

Table 2. Correlation linear (Pearson) matrix of terrestrial water storage and drought indices on the Senegalese regions.

	STI Zig	STI Ked	STI Tamba	STI Matam	SPI Ziguinchor	SPI Kédougou	SPI Mbour	SPI Tamba	SPI Dakar	SPI Matam	CSR	JPL	GSFC
STI Zig	**1**												
STI Ked	**0.64**	**1**											
STI Tamba	0.30	0.09	**1**										
STI Matam	**0.58**	0.48	**0.61**	**1**									
SPI Ziguinchor	0.42	**0.54**	0.20	0.36	**1**								
SPI Kédougou	−0.18	**−0.57**	0.26	0.10	0.03	**1**							
SPI Mbour	0.30	0.19	0.13	0.48	0.39	0.36	**1**						
SPI Tamba	−0.01	−0.31	0.00	−0.28	0.11	0.41	0.19	**1**					
SPI Dakar	0.19	0.22	0.17	0.20	**0.62**	0.35	**0.71**	0.13	**1**				
SPI Matam	−0.39	−0.39	−0.31	−0.29	−0.28	0.03	0.06	−0.17	−0.10	**1**			
CSR	0.34	**0.58**	0.45	**0.68**	0.39	0.01	0.16	−0.33	0.08	−0.20	**1**		
JPL	0.40	**0.70**	0.38	**0.71**	0.44	−0.12	0.18	−0.50	0.14	−0.19	**0.97**	**1**	
GSFC	0.45	**0.72**	0.28	**0.63**	0.51	−0.11	0.19	−0.39	0.18	−0.16	**0.94**	**0.97**	**1**

Values in bold denote correlations that are statistically significant at a 95% confidence level.

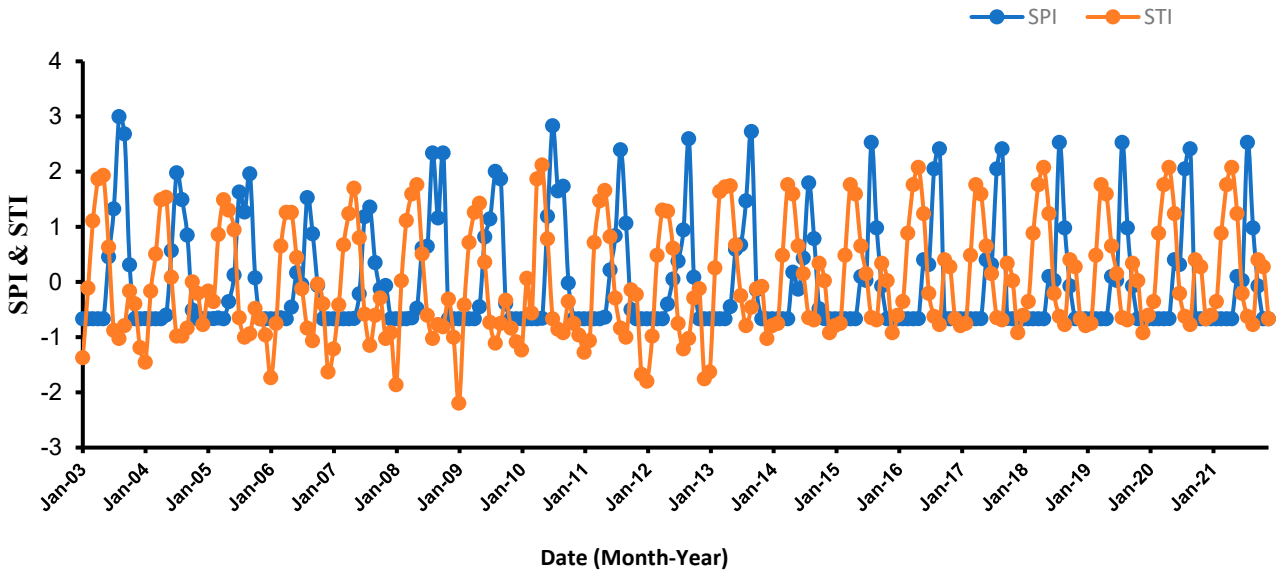

Figure 10. SPI and STI time series over the study area during the entire period.

The estimated linear (Pearson) correlations between water storage and climate indices are displayed in Table 2. At the 95% confidence level, the correlation coefficients show a

substantial association between water storage and other climate indicators, such as STI and SPI, as well as a consistent pattern of related inter-annual trends. The highest correlation coefficients for water storage in Senegal are discovered with STI in Matam (0.68 for CSR, 0.71 for JPL, and 0.63 for GSFC) and Kédougou when compared to meteorological indices (0.58 for CSR, 0.70 for JPL and 0.72 for GSFC). Only Ziguinchor had a significant connection between SPI and water storage (0.39 for CSR, 0.44 for JPL, and 0.51 for GSFC), with Mbour coming in second (0.16 for CSR, 0.18 for JPL, and 0.19 for GSFC), and Tambacounda and Matam having a negative correlation. Overall, significant correlations between standardized indicators of the same type have been found (for example, between storage indices on the three series of mascon data, the correlation coefficients are greater than 0.94).

Figures 2 and 5b reveal that substantial precipitation occurs between June and October, while high ΔTWS anomalies occur between August and November. The strongest ΔTWS response appears to lag Senegal's rainfall by two months. Similar findings have been published by [85,86], stating that the maximal GARCE-derived ΔTWS response lags precipitation by 1.5 to 2 months over the Lake Chad region. In the Northwestern Sahara Aquifer, the ΔTWS seasonal cycle lags precipitation by approximately 2 months and 10 days, whereas the ΔGWS seasonal cycle lags precipitation by approximately 3 months [87]. Given that the ΔGWS represents the groundwater reserve below the subsurface, it would appear that the strongest ΔGWS reaction occurs later than the ΔTWS and lags behind the heaviest rainfall by three months, as observed from Figures 5b and 7.

The NOAA National Geophysical Data Center provided the sediment thickness information for download [88]. The sediment thickness of Senegal shows an increase from less than 200 m at the mountainous region in the southeastern part to more than 8000 m (Figure 11) in the western part of the study area close to the coastal area. This distribution of the sediment thickness reflects the presence of higher reserves of groundwater in the western part of the country.

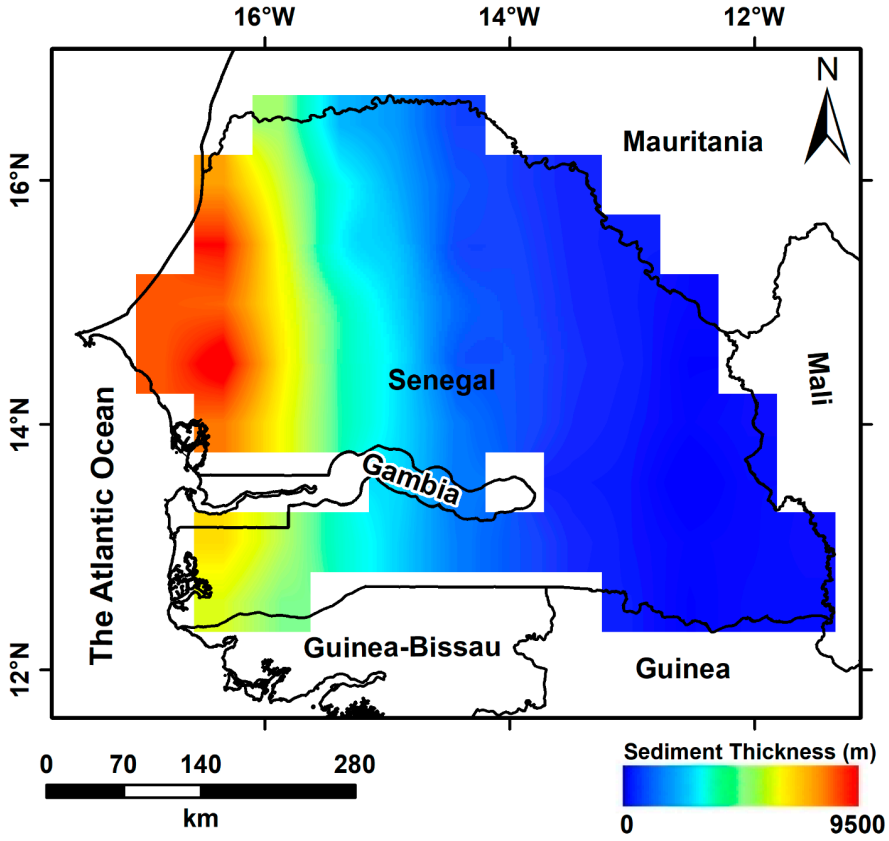

Figure 11. An illustration of the thickness of the sedimentary succession (m).

By combining the ΔGWS variation rate +0.63 ± 0.08 cm/yr (+1.24 ± 0.16 km^3/yr) and the artificial withdrawal rate (1.13 ± 0.11 cm/yr (2.22 ± 0.22 km^3/yr; FAO, 2022) during the research period, the country is receiving an average recharge rate of 1.76 ± 0.14 cm/yr (+3.46 ± 0.27 km^3/yr), we have added a 10% error for the artificial withdrawal rate. On the other hand, large hydrogeological environments, such as aquifer systems, have been evaluated for their recharge and depletion rates using physical, chemical, and modelling methodologies [89–92]. However, regional implementation of these methods is challenging because of a lack of requisite datasets, the time and effort required to obtain these data, and the sometimes-questionable quality of the conclusions they produce.

The country needs to manage surface and groundwater resources to protect its groundwater resources. Water diversion and groundwater protection must be regulated by law. The installation of small dams in the major streams helps to prevent surface water from entering the ocean and feeds the groundwater supply of groundwater aquifers.

6. Conclusions

GRACE offers an innovative approach to estimate the changes in terrestrial water storage on the territory of Senegal.

- At +0.63 ± 0.08 cm/yr, the average terrestrial water storage exhibits a positive increase trend over the study period.
- The fluctuations in groundwater storage are comparable to those of terrestrial water storage.
- Throughout the entire period, the groundwater storage has a generally positive trend of +0.63 ± 0.08 cm/yr, with Period III showing the highest trend value of +1.64 ± 1.11 cm/yr.
- Throughout the whole period, the research area has experienced an average yearly precipitation rate of 692.5 mm.
- In addition to SPI and STI, GRACE-based ΔTWS anomalies are useful indicators for tracking extreme hydrological events.
- Groundwater recharge is currently being seen in the country as a result of rising rainfall, according to GRACE-derived estimations of ΔTWS.
- The annual amplitude of groundwater in Senegal is 5.36 cm, with a positive trend of about 0.63 ± 0.08 cm/year (1.24 ± 0.16 km^3/yr) during the entire period.
- Throughout the entire era, the nation receives an annual recharge rate of +1.76 ± 0.14 cm/yr (+3.46 ± 0.28 km^3/yr).
- More effective procedures should be implemented to assess the increase in groundwater detected by GRACE in Senegal and observe any additional water-related activities to those already taking place.
- In general, the approach utilized in this article allowed for the estimation of groundwater storage variation as well as the identification of the most significant drought periods that have affected the Senegalese area.
- For large-scale areas, especially those where hydrometeorological sites are scarce or where the reliability of the available data is low, GRACE data can also be a perfect replacement. To improve the application's accuracy and coverage, the future investigation should concentrate on enhancing the methodology of ΔTWS indices and determining the severity of drought.

Author Contributions: Conceptualization, A.M.; Data curation, A.M. and C.F.; Formal analysis, A.M.; Investigation, A.M. and C.F.; Methodology, A.M. and C.F.; Project administration, A.M.; Resources, A.M., C.F., A.O. and A.A.; Software, A.M. and C.F.; Validation, A.M. and A.A.; Visualization, A.M., A.A. and A.O.; Writing—original draft, C.F. and A.M.; Writing—review & editing, A.M. All authors have read and agreed to the published version of the manuscript.

Funding: This research received no external funding.

Data Availability Statement: The data is available upon request from the authors.

Conflicts of Interest: The authors declare no conflict of interest.

References

1. FAO 2022. AQUASTAT Website. Food and Agriculture Organization of the United Nations. Available online: http://www.fao.org/statistics/fr/ (accessed on 26 June 2022).
2. CONGAD. Blue Book "Water, Life, Human Development" Country Report: Senegal, Consultation Document Provided by Senagrosol Consult; 2009; p. 72.
3. Faye, C.; Gomis, E.N.; Dieye, S. Current situation and sustainable development of water resources in Senegal. *Ecol. Eng. Environ. Prot.* **2019**, *1*, 5–16. [CrossRef]
4. Faye, C.; Dieye, S. Valorization of water resources in Senegal for economic, social and sustainable development. *Afr. J. Environ. Sci. Technol.* **2018**, *12*, 449–460.
5. Sow, A.A. L'hydrologie du Sud-est du Sénégal et de ses Confins Guinéo-Maliens: Les Bassins de la GAMBIE et de la Falémé. Ph.D. Thesis, Université Cheikh Anta Diop de Dakar, Dakar, Senegal, 2007; p. 1232.
6. Faye, C. Evaluation and Integrated Management of Water Resources in a Context of Hydroclimatic Variability: Case of the Falémé Watershed. Ph.D. Thesis, Cheikh Anta Diop University of Dakar, Dakar, Senegal, 2013; p. 309.
7. Faye, C.; Sow, A.A.; Ndong, J.B. Study of rainfall and hydrological droughts in tropical Africa: Characterization and mapping of drought by indices in the upper Senegal River basin. *Physio-Geo-Phys. Geogr. Environ.* **2015**, *9*, 17–35.
8. Faye, C. Characterisation of low water: The lasting effects of rainfall deficit on low water and drying up in the Bakoye basin. *Espaces Soc. Mutat. Spec. Issue* **2015**, 109–126.
9. Faye, C.; Diop, E.S.; Mbaye, I. Impacts of climate change and development on the water resources of the Senegal River: Characterization and evolution of hydrological regimes of natural and developed sub-catchments. *Belgeo* **2015**, *4*, 1–22.
10. Faye, C. Variability and trends observed in monthly, seasonal and annual mean flows in the Falémé River basin (Senegal). *Hydrol. Sci. J. J. Des Sci. Hydrol.* **2017**, *62*, 259–269. [CrossRef]
11. Dai, A.G. Drought under global warming: A review. *Adv. Rev.* **2011**, *2*, 45–65. [CrossRef]
12. Zhao, Q.; Wu, W.W.; Wu, Y.L. Variations in China's terrestrial water storage over the past decade using GRACE data. *Geod. Geodyn.* **2015**, *6*, 187–193. [CrossRef]
13. Döll, P.; Jiménez-Cisneros, B.; Oki, T.; Arnell, N.W.; Benito, G.; Cogley, J.G.; Jiang, T.; Kundzewicz, Z.W.; Mwakalila, S.; Nishijima, A. Integrating risks of climate change into water management. *Hydrol. Sci. J.* **2014**, *60*, 4–13. [CrossRef]
14. Tapley, B.D.; Bettadpur, S.; Ries, J.C.; Thompson, P.F.; Watkins, M. GRACE measurements of mass variability in the Earth system. *Science* **2004**, *305*, 503–505. [CrossRef]
15. Wahr, J.; Swenson, S.; Zlotnicki, V.; Velicogna, I. Time-variable gravity from GRACE: First results. *Geophys. Res. Lett.* **2004**, *31*, L11501. [CrossRef]
16. Rodell, M.; Famiglietti, J.S.; Chen, J.; Seneviratne, S.I.; Viterbo, P.; Holl, S.; Wilson, C.R. Basin scale estimates of evapotranspiration using GRACE and other observations. *Geophys. Res. Lett.* **2004**, *31*, L20504. [CrossRef]
17. Girotto, M.; Rodell, M. Chapter Two—Terrestrial water storage. In *Extreme Hydroclimatic Events and Multivariate Hazards in a Changing Environment*; Maggioni, V., Massari, C., Eds.; Elsevier: Amsterdam, The Netherlands, 2019; pp. 41–64. ISBN 9780128148990. [CrossRef]
18. Ramillien, G.; Frappart, F.; Cazenave, A.; Güntner, A. Time variations of land water storage from an inversion of 2 years of GRACE geoids. *Earth Planet. Sci. Lett.* **2005**, *235*, 283–301. [CrossRef]
19. Davis, J.L.; Elósegui, P.; Mitrovica, J.X.; Tamisiea, M.E. Climate-driven deformation of the solid Earth from GRACE and GPS. *Geophys. Res. Lett.* **2004**, *31*, L24605. [CrossRef]
20. Yeh, P.J.; Swenson, S.C.; Famiglietti, J.S.; Rodell, M. Remote sensing of groundwater storage changes in Illinois using the gravity recovery and climate experiment (GRACE). *Water Resour. Res.* **2006**, *42*, 1–7. [CrossRef]
21. Castellazzi, P.; Longuevergne, L.; Martel, R.; Rivera, A.; Brouard, C.; Chaussard, E. Quantitative mapping of groundwater depletion at the water management scale using a combined GRACE/InSAR approach. *Remote Sens. Environ.* **2018**, *205*, 408–418. [CrossRef]
22. Yan, H.; Wang, S.; Wang, J.; Lu, H.; Guo, A.; Zhu, Z.; Myneni, R.; Shugart, H. Assessing spatiotemporal variation of drought in China and its impact on agriculture during 1982–2011 by using PDSI indices and agriculture drought survey data. *J. Geophys. Res.* **2016**, *121*, 2283–2298. [CrossRef]
23. Heim, R.R. A review of twentieth-century drought indices used in the United States. *Bull. Am. Meteorol. Soc.* **2002**, *83*, 1149–1165. [CrossRef]
24. Ni, S.; Chen, J.; Wilson, C.R.; Li, J.; Hu, X.; Fu, R. Global terrestrial water storage changes and connections to ENSO events. *Surv. Geophys.* **2018**, *39*, 1–22. [CrossRef]
25. Anyah, R.O.; Forootan, E.; Awange, J.L.; Khaki, M. Understanding linkages between global climate indices and terrestrial water storage changes over Africa using GRACE products. *Sci. Total Environ.* **2018**, *635*, 1405–1416. [CrossRef] [PubMed]

26. Ndehedehe, C.E.; Awange, J.L.; Corner, R.J.; Kuhn, M.; Okwuashi, O. On the potentials of multiple climate variables in assessing the spatio-temporal chracterstics of hydrological droughts over the Volta Basin. *Sci. Total Environ.* **2016**, *557–558*, 819–837. [CrossRef] [PubMed]
27. Seyoum, W.M. Characterizing water storage trends and regional climate influence using GRACE observation and satellite altimetry data in the Upper Blue Nile River Basin. *J. Hydrol.* **2018**, *566*, 274–284. [CrossRef]
28. Scanlon, B.R.; Longuevergne, L.; Long, D. Ground referencing GRACE satellite estimates of groundwater storage changes in the California Central Valley, USA. *Water Resour. Res.* **2012**, *48*, W04520. [CrossRef]
29. Ferreira, V.G.; Gong, Z.; Andam-Akorful, S.A. Monitoring mass changes in the volta river basin using GRACE satellite gravity and TRMM precipitation. *Bol. Cienc. Geod.* **2012**, *18*, 549–563. [CrossRef]
30. Richey, A.S.; Thomas, B.F.; Lo, M.-H.; Reager, J.T.; Famiglietti, J.S.; Voss, K.; Swenson, S.; Rodell, M. Quantifying renewable groundwater stress with GRACE. *Water Resour. Res.* **2015**, *51*, 5217–5238. [CrossRef]
31. Mohamed, A.; Sultan, M.; Ahmed, M.; Yan, E.; Ahmed, E. Aquifer recharge, depletion, and connectivity: Inferences from GRACE, land surface models, and geochemical and geophysical data. *Bull. Geol. Soc. Am.* **2017**, *129*, 534–546. [CrossRef]
32. Rodell, M.; Famiglietti, J.S.; Wiese, D.N.; Reager, J.T.; Beaudoing, H.K.; Landerer, F.W.; Lo, M.-H. Emerging trends in global freshwater availability. *Nature* **2018**, *557*, 651–659. [CrossRef]
33. Fallatah, O.A.; Ahmed, M.; Cardace, D.; Boving, T.; Akanda, A.S. Assessment of modern recharge to arid region aquifers using an integrated geophysical, geochemical, and remote sensing approach. *J. Hydrol.* **2019**, *569*, 600–611. [CrossRef]
34. Mohamed, A. Hydro-geophysical study of the groundwater storage variations over the Libyan area and its connection to the Dakhla basin in Egypt. *J. Afr. Earth Sci.* **2019**, *157*, 103508. [CrossRef]
35. Mohamed, A. Gravity based estimates of modern recharge of the Sudanese area. *J. Afr. Earth Sci.* **2020**, *163*, 103740. [CrossRef]
36. Mohamed, A. Gravity applications in estimating the mass variations in the Middle East: A case study from Iran. *Arab. J. Geosci.* **2020**, *13*, 364. [CrossRef]
37. Mohamed, A. Gravity applications to groundwater storage variations of the Nile Delta Aquifer. *J. Appl. Geophys.* **2020**, *182*, 104177. [CrossRef]
38. Mohamed, A.; Ragaa Eldeen, E.; Abdelmalik, K. Gravity based assessment of spatio-temporal mass variations of the groundwater resources in the Eastern Desert, Egypt. *Arab. J. Geosci.* **2021**, *14*, 500. [CrossRef]
39. Mohamed, A.; Abdelrahman, K.; Abdelrady, A. Application of Time- Variable Gravity to Groundwater Storage Fluctuations in Saudi Arabia. *Front. Earth Sci.* **2022**, *10*, 873352. [CrossRef]
40. Mohamed, A.; Al Deep, M.; Othman, A.; Taha Al Alshehri, F.; Abdelrady, A. Integrated geophysical assessment of ground-water potential in southwestern Saudi Arabia. *Front. Earth Sci.* **2022**, *10*, 937402. [CrossRef]
41. Taha, A.I.; Al Deep, M.; Mohamed, A. Investigation of groundwater occurrence using gravity and electrical resistivity methods: A case study from Wadi Sar, Hijaz Mountains, Saudi Arabia. *Arab. J. Geosci.* **2021**, *14*, 334. [CrossRef]
42. Mohamed, A.; Gonçalvès, J. Hydro-geophysical monitoring of the North Western Sahara Aquifer System's groundwater resources using gravity data. *J. Afr. Earth Sci.* **2021**, *178*, 104188. [CrossRef]
43. Othman, A.; Abdelrady, A.; Mohamed, A. Monitoring Mass Variations in Iraq Using Time-Variable Gravity Data. *Remote Sens.* **2022**, *14*, 3346. [CrossRef]
44. Andam-Akorful, S.A.; Ferreira, V.G.; Awange, J.L.; Forootan, E.; He, X.F. Multi-model and multi-sensor estimations of evapotranspiration over the Volta Basin, West Africa. *Int. J. Climatol.* **2015**, *35*, 3132–3145. [CrossRef]
45. Li, B.; Rodell, M.; Zaitchik, B.F.; Reichle, R.H.; Koster, R.D.; van Dam, T.M. Assimilation of GRACE terrestrial water storage into a land surface model: Evaluation and potential value for drought monitoring in western and central Europe. *J. Hydrol.* **2012**, *446–447*, 103–115. [CrossRef]
46. Rodell, M.; Velicogna, I.; Famiglietti, J.S. Satellite-based estimates of groundwater depletion in India. *Nature* **2009**, *460*, 999–1002. [CrossRef] [PubMed]
47. Moiwo, J.P.; Tao, F.; Lu, W. Estimating soil moisture storage change using quasi-terrestrial water balance method. *Agric. Water Manag.* **2011**, *102*, 25–34. [CrossRef]
48. Long, D.; Shen, Y.J.; Sun, A.; Hong, Y.; Longuevergne, L.; Yang, Y.T.; Li, B.; Chen, L. Drought and flood monitoring for a large karst plateau in southwest China using extended GRACE data. *Remote Sens. Environ.* **2014**, *155*, 145–160. [CrossRef]
49. Thomas, A.C.; Reager, J.T.; Famiglietti, J.S.; Rodell, M. A GRACE based water storage deficit approach for hydrological drought characterization. *Geophys. Res. Lett.* **2014**, *41*, 1537–1545. [CrossRef]
50. Zhang, Y.; Yao, L.; Jing, G.; Gaopeng, L.; Zhisheng, Y.; Haishan, N. Correlation analysis between drought indices and terrestrial water storage from 2002 to 2015 in China. *Environ. Earth Sci.* **2018**, *77*, 462. [CrossRef]
51. Nie, N.; Zhang, W.; Zhang, Z.; Guo, H.; Ishwaran, N. Reconstructed terrestrial water storage change (ΔTWS) from 1948 to 2012 over the Amazon Basin with the latest GRACE and GLDAS products. *Water Resour. Manag.* **2016**, *30*, 279–294. [CrossRef]
52. Tang, J.S.; Cheng, H.W.; Liu, L. Assessing the recent droughts in southwestern China using satellite gravimetry. *Water Resour. Res.* **2014**, *50*, 3030–3038. [CrossRef]
53. Cao, Y.P.; Nan, Z.T.; Cheng, G.D. GRACE gravity satellite observations of terrestrial water storage changes for drought characterization in the arid land of Northwestern China. *Remote Sens.* **2015**, *7*, 1021–1047. [CrossRef]
54. Vicente-Serrano, S.; van der Schrier, G.; Beguería, S.; Azorin-Molina, C.; Lopez-Moreno, J. Contribution of precipitation and reference evapotranspiration to drought indices under different climates. *J. Hydrol.* **2015**, *526*, 42–54. [CrossRef]

55. Zhao, M.; Velicogna, A.G.R.; Kimball, I.J.S. Satellite observations of regional drought severity in the continental United States using GRACE-based terrestrial water storage changes. *J. Clim.* **2017**, *30*, 6297–6308. [CrossRef]
56. Sane, M. *Note Sur Les Ressources en Eaux du Sénégal: Zones potentielles Pour le Transfert D'eau*; Directeur de l'hydraulique: République du Sénégal, Senegal, 2015; p. 8.
57. Luthcke, S.B.; Sabaka, T.J.; Loomis, B.D.; Arendt, A.A.; McCarthy, J.J.; Camp, J. Antarctica, Greenland, and Gulf of Alaska land-ice evolution from an iterated GRACE global mascon solution. *J. Glaciol.* **2013**, *59*, 216. [CrossRef]
58. Watkins, M.M.; Wiese, D.N.; Yuan, D.-N.; Boening, C.; Landerer, F.W. Improved methods for observing Earth's time variable mass distribution with GRACE using spherical cap mascons. *J. Geophys. Res. Solid Earth* **2015**, *120*, 2648–2671. [CrossRef]
59. Wiese, D.N.; Landerer, F.W.; Watkins, M.M. Quantifying and reducing leakage errors in the JPL RL05M GRACE mascon solution. *Water Resour. Res.* **2016**, *52*, 7490–7502. [CrossRef]
60. Save, H.; Bettadpur, S.; Tapley, B. High-resolution CSR GRACE RL05 mascons. *J. Geophys. Res. Solid Earth* **2016**, *121*, 7547–7569. [CrossRef]
61. Save, H. CSR GRACE and GRACE-FO RL06 Mascon Solutions v02. *Mascon Solut.* **2020**, *12*, 24.
62. Loomis, B.D.; Luthcke, S.B.; Sabaka, T.J. Regularization and error characterization of GRACE mascons. *J. Geod.* **2019**, *93*, 1381–1398. [CrossRef]
63. Yirdaw, S.Z.; Snelgrove, K.R.; Agboma, C.O. GRACE satellite observations of terrestrial moisture changes for drought characterization in the Canadian Prairie. *J. Hydrol.* **2008**, *356*, 84–92. [CrossRef]
64. Rodell, M.; Houser, P.R.; Jambor, U.; Gottschalck, J.; Mitchell, K.; Meng, C.-J.; Arsenault, K.; Cosgrove, B.; Radakovich, J.; Bosilovich, M.; et al. The global land data Assimilation system. *Bull. Am. Meteorol. Soc.* **2004**, *85*, 381–394. [CrossRef]
65. Kummerow, C.; Barnes, W.; Koju, T.; Shiue, J.; Simpson, J. The Tropical Rainfall Measuring Mission (TRMM) Sensor Package. *J. Atmos. Ocean. Technol.* **1998**, *15*, 809–817. [CrossRef]
66. McKee, T.B.; Doesken, N.J.; Kleist, J. The relationship of drought frequency and duration to time scales. In Proceedings of the 8th Conference on Applied Climatology, Boston, MA, USA, 17–22 January 1993; American Meteorological Society: Anaheim, CA, USA, 1993; pp. 179–186.
67. Hayes, M.J.; Svoboda, M.D.; Wilhite, D.A.; Vanyarkho, O.V. Monitoring the 1996 drought using the standardized precipitation index. *Bull. Am. Meteorol. Soc.* **1999**, *80*, 429–438. [CrossRef]
68. Li, B.; Rodell, M.; Famiglietti, J.S. Groundwater variability across temporal and spatial scales in the central and northeastern U.S. *J. Hydrol.* **2015**, *525*, 769–780. [CrossRef]
69. Famiglietti, J.S. The global groundwater crisis. *Nat. Clim. Change* **2014**, *4*, 945–948. [CrossRef]
70. Famiglietti, J.S.; Cazenave, A.; Eicker, A.; Reager, J.T.; Rodell, M.; Velicogna, I. Satellites provide the big picture. *Science* **2015**, *349*, 684–685. [CrossRef]
71. Döll, P. Vulnerability to the impact of climate change on renewable groundwater resources: A global-scale assessment. *Environ. Res. Lett.* **2009**, *4*, 035006. [CrossRef]
72. Thomas, B.F.; Caineta, J.; Nanteza, J. Global assessment of groundwater sustainability based on storage anomalies. *Geophys. Res. Lett.* **2017**, *44*, 1–11. [CrossRef]
73. Rosegrant, M.W.; Ringler, C.; Zhu, T. Water for agriculture: Maintaining food security under growing scarcity. *Annu. Rev. Environ. Resour.* **2009**, *34*, 205–222. [CrossRef]
74. Connor, R. *The United Nations World Water Development Report 2015: Water for a Sustainable World*; UNESCO Publishing: France, Paris, 2015; Volume 1, p. 122.
75. Zhangli, S.; Xiufang, Z.; Yaozhong, P.; Jinshui, Z.; Xianfeng, L. Drought evaluation using the GRACE terrestrialwater storage deficit over the Yangtze River Basin, China. *Sci. Total Environ.* **2018**, *634*, 727–738.
76. Feng, W. Regional Variations in Terrestrial Water Storage and Sea Level Detected by Spatial Gravimetry. Ph.D. Thesis, University Toulouse 3 Paul Sabatier (UT3 Paul Sabatier), Toulouse, France, 2014; p. 140.
77. Emerton, R.E.; Stephens, E.M.; Pappenberger, F.; Pagano, T.C.; Weerts, A.H.; Wood, A.W.; Salamon, P.; Brown, J.D.; Hjerdt, N.; Donnelly, C.; et al. Continental and global scale flood forecasting systems. *Wiley Interdiscip. Rev. Water* **2016**, *3*, 391–418. [CrossRef]
78. Chen, J.L.; Wilson, C.R.; Seo, K.W. Optimized smoothing of gravity recovery and climate experiment (grace) time-variable gravity observations. *J. Geophys. Res. Solid Earth* **2006**, *111*, 408. [CrossRef]
79. Duan, X.J.; Guo, J.Y.; Shum, C.K.; van der Wal, W. On the postprocessing removal of correlated errors in GRACE temporal gravity field solutions. *J. Geod.* **2009**, *83*, 1095–1106. [CrossRef]
80. Mohamed, A.; Al Deep, M. Depth to the bottom of the magnetic layer, crustal thickness, and heat flow in Africa: Inferences from gravity and magnetic data. *J. Afr. Earth Sci.* **2021**, *179*, 104204. [CrossRef]
81. Mohamed, A.; Al Deep, M.; Abdelrahman, K.; Abdelrady, A. Geometry of the Magma Chamber and Curie Point Depth Beneath Hawaii Island: Inferences from Magnetic and Gravity Data. *Front. Earth Sci. Sect. Solid Earth Geophys.* **2022**, *10*, 847984. [CrossRef]
82. Othman, A. Measuring and Monitoring Land Subsidence and Earth Fissures in Al-Qassim Region, Saudi Arabia: Inferences from InSAR. In *Advances in Remote Sensing and Geo Informatics Applications*; El-Askary, H., Lee, S., Heggy, E., Pradhan, B., Eds.; Springer: Cham, Switzerland, 2019; pp. 287–291. [CrossRef]
83. AL Deep, M.; Araffa, S.A.S.; Mansour, S.A.; Taha, A.I.; Mohamed, A.; Othman, A. Geophysics and remote sensing applications for groundwater exploration in fractured basement: A case study from Abha area, Saudi Arabia. *J. Afr. Earth Sci.* **2021**, *184*, 104368. [CrossRef]

84. Mohamed, A.; Abu El Ella, E.M. Magnetic Applications to Subsurface and Groundwater Investigations: A Case Study from Wadi El Assiuti, Egypt. *Int. J. Geosci.* **2021**, *12*, 77–101. [CrossRef]
85. Buma, W.G.; Lee, S.-I.; Seo, J.Y. Hydrological Evaluation of Lake Chad Basin Using Space Borne and Hydrological Model Observations. *Water* **2016**, *8*, 205. [CrossRef]
86. Skaskevych, A.; Lee, J.; Jung, H.C.; Bolten, J.; David, J.L.; Policelli, F.S.; Goni, I.B.; Favreau, G.; San, S.; Ichoku, C.M. Application of GRACE to the estimation of groundwater storage change in a data-poor region: A case study of Ngadda catchment in the Lake Chad Basin. *Hydrol. Process.* **2020**, *34*, 941–955. [CrossRef]
87. Gonçalvès, J.; Petersen, J.; Deschamps, P.; Hamelin, B.; Baba-Sy, O. Quantifying the modern recharge of the "fossil" Sahara aquifers. *Geophys. Res. Lett.* **2013**, *40*, 2673–2678. [CrossRef]
88. Divins, D. *Total Sediment Thickness of the World's Oceans and Marginal Seas*; NOAA National Geophysical Data Center: Boulder, CO, USA, 2003.
89. de Vries, J.J.; Simmers, I. Groundwater recharge: An overview of process and challenges. *Hydrogeol. J.* **2002**, *10*, 5–17. [CrossRef]
90. Milewski, A.; Sultan, M.; Yan, E.; Becker, R.; Abdeldayem, A.; Soliman, F.; Gelil, K.A. A remote sensing solution for estimating runoff and recharge in arid environments. *J. Hydrol.* **2009**, *373*, 1–14. [CrossRef]
91. Mohamed, A.; Ahmed, E.; Alshehri, F.; Abdelrady, A. The groundwater flow behavior and the recharge in the Nubian Sandstone Aquifer System during the wet and arid periods. *Sustainability* **2022**, *14*, 6823. [CrossRef]
92. Mohamed, A.; Asmoay, A.; Alshehri, F.; Abdelrady, A.; Othman, A. Hydro-geochemical applications and multivariate analysis to assess the water–rock interaction in arid environments. *Appl. Sci.* **2022**, *12*, 6340. [CrossRef]